Electronic Journal of Structural Engineering

Original Article

Cite this: DOI:10.56748/ejse.23433

Received Date: 10 March 2023
Accepted Date: 11 October 2023

1443-9255
https://ejsei.com/ejse

Seismic Assessment of High-Rise Buildings Having Transfer Elements

E.Z. El-Bayome*, A. M. Abd El-Salam, O. O. El-Mahdy, H. M. Refat
Faculty of Engineering, Benha University, Egypt.
*Corresponding author: sayed.zakria@bhit.bu.edu.eg

Abstract

This paper investigates the seismic behavior of high-rise buildings having transfer elements. Three constructed reinforced concrete (RC) buildings having either transfer slabs or transfer girders were analyzed using the response spectrum (RS) and time-history (TH) methods. For each building, the story shear, bending moment, displacement, drift, and time period were obtained. Furthermore, pushover analysis (POA) method was conducted to evaluate the capability of these buildings to resist the expected seismic loads. Results of the studied buildings showed that, the base shears obtained using pushover analysis are ranging between 50% to 83% of those calculated using the static approach. In addition, the response modification factors (R) for these buildings were calculated to show their sensitivity due to the irregularity of buildings. For the studied cases in this research, the R values given in the building codes were overestimated for the cases with transfer slabs and underestimated for cases with transfer girders.

Keywords

High-rise buildings, Transfer elements, Response spectrum, Time-history, Pushover analysis

1. Introduction

Nowadays, economic power and leadership are manifested by high-rise buildings. Thus, there exists a worldwide competition in having the highest building. Innovative structural systems such as discontinuous vertical elements are needed to satisfy the demands of architectural design. Currently, many high-rise buildings are constructed with vertical irregularity system, where the transfer elements are used to transmit vertical and lateral loads from discontinuous columns and walls to the below structural elements.

Several researchers investigated the structural behavior of tall buildings having transfer elements. (Londhe, 2011) conducted an experimental study to investigate the shear capacity of reinforced concrete transfer beams. Moreover, the author suggested an analytical model to design transfer beams in tall buildings. (Elawady, et al., 2014) performed a comparison study for the seismic response of high-rise buildings with transfer slabs and girders. The analysis indicated that the position of damage was in the vicinity of the transfer floor and the first floor. (Abdelbasset, et al., 2014) studied the effect of transfer floors on the drift of the building. The transfer floor system comprised of solid transfer plates located at 20% of the total building height. The analysis was carried out using reduced stiffness of different structural elements, in addition to using full stiffness for all elements. The analytical results revealed that stiffness reduction of vertical and horizontal elements had significantly affected the drift and lateral displacements by about 30%. (Osman & Abdel Azim, 2015) investigated the behavior of high-rise buildings with thick transfer slabs. Results of the analytical models depicted that neglecting the interaction between the transfer floor and the structural elements of the tower led to incorrect estimation of the straining actions. (Yacoubian, et al., 2017) studied the seismic shear demands on tower walls supporting high-rise buildings. They addressed the displacement incompatibility between connected walls that imposed high in-plane strains in the slabs and beams connecting the tower wall above the podium interface level. It was found that podium can impose different boundary conditions on tower walls with respect to their proximity to the center of the podium or the location along the supporting transfer plate. (Elassaly & Nabil, 2017) inspected seismic behavior of two dimensional reinforced concrete structures using transfer slab models. In their research, six natural ground motions were used. It was concluded that the transfer slab led to an increase in the story shear in podium portion and in the level containing transfer slab. (Abdul Sameer & Azeem, 2019) postulated a study on the seismic behavior of high-rise building with transfer floors. Models of three buildings using moment resisting frame (MRF) and shear wall frame (SWF) were studied. Results of MRF models highlighted good results for the transfer slab located at the lower level. SWF models showed better performance in both, stiffness and load capacity leading to better results for base shear, story drift, and roof displacement. (Ayash, et al., 2020) examined the seismic performance of tall buildings having two transfer slabs. Six cases of transfer floors locations were studied. Seismic loads were applied using nonlinear time history analysis of three scaled earthquakes. It was postulated that the worst seismic performance was for the building having two transfer floors at lower levels and nearer space between transfer slabs.

2. Design Guidelines of Codes

The (UBC 97, 1997) and (ASCE 7, 2010) codes establish fundamental load combinations applicable to conventional buildings. However, for irregular buildings, distinct special load combinations are outlined, accounting for both allowable stress and strength design methods, as follows:

$$\text{UBC 1997:} \qquad \begin{matrix} 1.2D + f_1 L + 1.0E_m \\ 0.9D + 1.0E_m \end{matrix} \qquad (1)$$

Where, the factorf_1 takes the value of 1.0 for public assembly and/or garage floors and for live loads exceeding 4.79 kN/m2, and it is set to 0.5 for other live loads. D represents the dead load, while E_m denotes the estimated maximum earthquake force achievable within the structure; Em is calculated as $\Omega_o E_h$, with Ω_o representing the seismic force amplification factor required to consider structural over-strength (Ω_o ranging from 2.0 to 2.8), and E_h indicating the earthquake load.

$$\text{ASCE7-10:} \qquad \begin{matrix} (1.2 + 0.2S_{Ds}) + E_{mh} + L + 0.2S \\ (0.9 - 0.2S_{Ds}) + E_{mh} + 1.6H \end{matrix} \qquad (2)$$

In this context, D, S, and H correspond to the dead load, snow load, and lateral earth or water pressure, respectively. E_{mh} signifies the impact of horizontal seismic forces, encompassing the structural over-strength factor; E_{mh} is determined as $\Omega_o Q_E$, where Ω_o represents the seismic force amplification factor (ranging from 1.25 to 3.0) and Q_E signifies the horizontal seismic forces derived from V or FP (equivalent lateral force procedure). SDS denotes the design spectral response acceleration parameter at short periods.

3. Pushover Analysis Methods

Pushover analysis (POA) is a nonlinear static analysis method; where a structure subjected to gravity loading and a lateral load pattern is controlled by monotonic displacement that continuously increases until an ultimate condition is reached by elastic and inelastic behavior (FEMA-440, 2005). Pushover analysis methods are classified into three broad categories: conventional POA methods, adaptive POA methods, and energy based POA methods. Conventional POA methods used in this research are as follows: Capacity Spectrum Method (CSM) (Freeman , et al., 1975), N2 Method (Eurocode 8 (EC8-1), 2004) and (Stefano & Mariani, 2014), and Displacement Coefficient Method (DCM) (FEMA-356, 2000).

4. Performance-Based Design

Performance-based design is used by designers to evaluate the performance level of a building. Four levels of seismic performance were chosen as a basis for design as given in FEMA 356 that comprises Operational (O), Immediate Occupancy (IO), Life Safety (LS), and Collapse Prevention (CP). The force-displacement curve that gives the behavior of global structure against lateral load is shown in Fig. 1 (Hakim, et al., 2014). The performance limits can be classified into two primary categories: (1) global/structural limits and (2) local/element limits (ATC 40, 1996). The global limits encompass prerequisites for gravity load capacity, lateral load resistance, and lateral deformation. In situations where an element's capacity to bear gravity load diminishes, the structure must possess the capability to redistribute the load to other elements. The building system's lateral load resistance should not deteriorate by more than 20% of the structure's maximum resistance. Lateral deformations must adhere to the deformation limits outlined in Table 1. The utmost drift is defined as the inter-story drift at the performance point displacement.

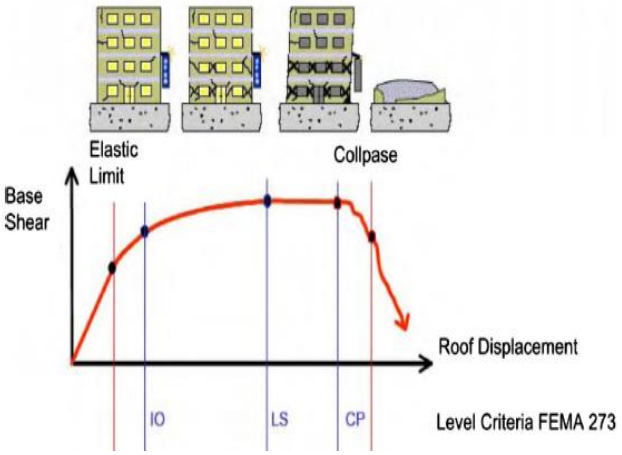

Fig. 1. Performance-based design (Hakim, et al., 2014).

Table 1. Deformation limits for each performance levels (ATC 40, 1996).

Immediate occupancy	Damage control	Life safety	Structural stability
0.01	0.01-0.02	0.02	0.33Vi/Pi

Element limits are frequently influenced by both nonstructural factors and component damage. The regulations imposed on the behavior of structural elements, like beams and columns, are grounded in their plastic hinge rotation capacities. This can be observed in Tables 2 and 3, which illustrate the deformation limits as per (ATC 40, 1996), using plastic hinge rotations for beam, column and walls elements within a reinforced concrete moment-resisting framework. Thus, it's essential to ascertain that member failure due to flexural demands and shear failure doesn't transpire before these predefined rotation limits are attained.

bending moment, displacement, drift, and time period were obtained. Furthermore, POA method is used to evaluate the capability of the existing building to resist expected seismic effects owing to the necessity of controlling the failure of irregular tall structures during earthquakes. In the POA, concrete and steel reinforcement materials are modeled using the isotropic unconfined stress-strain and uniaxial stress-strain relationships, respectively. Deformation controlled behavior is used for beam, frame, and wall elements with types of moment M3, interaction P-M2-M3, and fiber P-M3, respectively.

5. Case Studies

Three high-rise buildings which have already been designed and constructed in Egypt, KSA and UAE are chosen as case studies. Two of these buildings have transfer slabs, whereas the third one has transfer girders. Three-dimensional finite element models for these buildings are developed using ETABS computer program. Each building is analyzed using the RS and TH methods. The selected earthquakes in TH analysis were El-Centro 1940, Kobe 1995, and Northridge 1994. These earthquakes were matched with the corresponding response spectrum curve. Time-history of earthquakes used in this study are shown in and Fig. 2. These time histories are downloaded from Peer strong motion database (Peer Database, 2006).

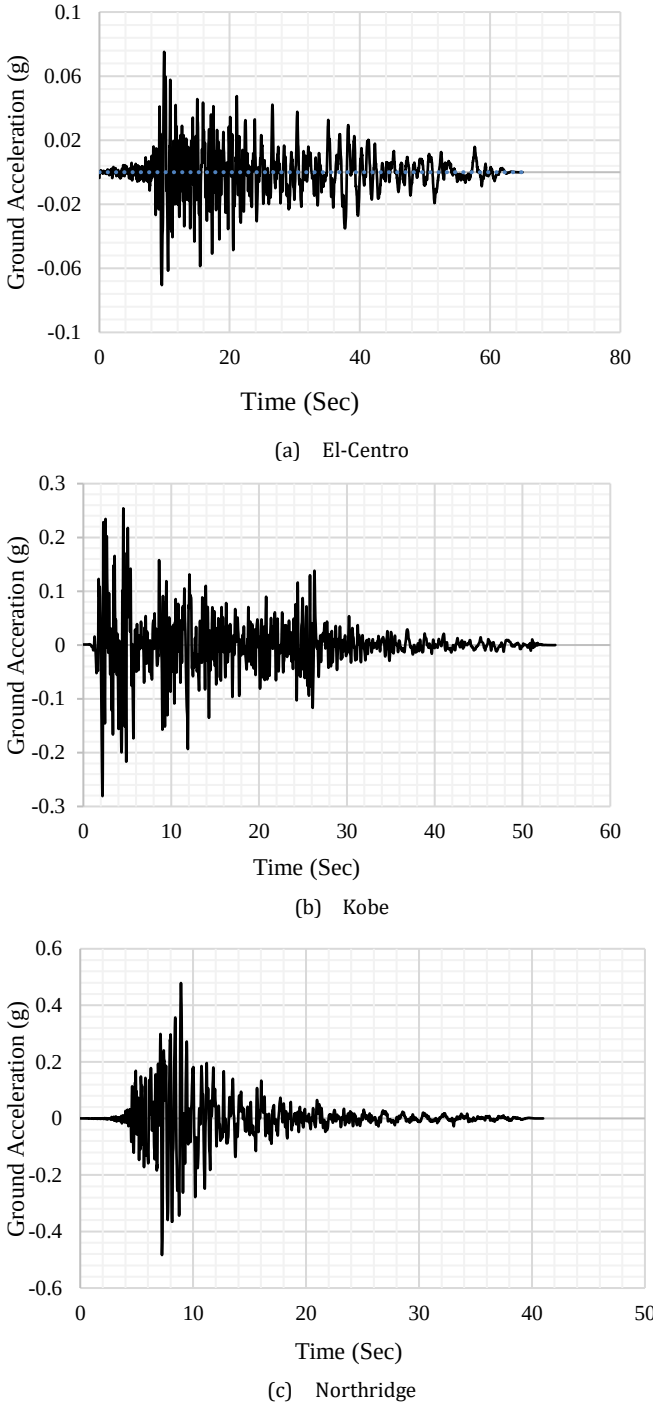

Fig. 2. Acceleration records of El-Centro, Kobe and Northridge earthquakes.

5.1 Study Case No. 1

This reinforced concrete building which constructed in in Cairo, Egypt, has three basements+ground+36 floors with a total height of 136.10 m above the ground level. The building was designed according to ECP201 and ECP203 codes. The developed 3D model is shown in Fig. 3. The main system resisting lateral loads is the building frame system and RC bracing. A reinforced concrete transfer slab with 2000 mm thick is located at 6th floor which is equal to 21% of the building total height. columns below and above transfer slab are shown in Figs. 4-5. It should be mentioned here that the structure has two cores starting from the foundation level, but the right core and the area of floor are reduced in dimension as shown in Fig. 3. The concrete compressive strength for both horizontal and vertical elements were 50 and 60 MPa, respectively. The yield stress for steel reinforcement was 400 MPa.

Table 2. Plastic rotation limits for RC beams controlled by flexure (ATC-40) (ATC 40, 1996).

$\rho - \rho^{\setminus}/\rho_{bal}$	Trans.Reinf.	$V/(b_\omega d\sqrt{fc})$	Modeling parameter			Plastic rotation limit		
			a	b	c	Immediate occupancy	Life safety	Structural stability
≤0.0	C	≤3.0	0.025	0.05	0.2	0.010	0.020	0.025
≤0.0	C	≥6.0	0.020	0.04	0.2	0.005	0.010	0.020
≥0.5	C	≤3.0	0.020	0.03	0.2	0.005	0.010	0.020
≥0.5	C	≥6.0	0.015	0.02	0.2	0.005	0.005	0.015

Table 3. Plastic rotation limits for RC Columns and walls controlled by flexure (ATC-40) [18].

$\rho - \rho^{\setminus}/\rho_{bal}$	Trans.Reinf.	$V/(b_\omega d\sqrt{fc})$	Modeling parameter			Plastic rotation limit		
			a	b	c	Immediate occupancy	Life safety	Structural stability
≤ 0.1	C	≤3.0	0.02	0.03	0.2	0.005	0.010	0.020
≤ 0.1	C	≥6.0	0.016	0.024	0.2	0.005	0.010	0.015
≥ 0.4	C	≤3.0	0.015	0.025	0.2	0.003	0.005	0.015
≥ 0.4	C	≥6.0	0.012	0.02	0.2	0.003	0.005	0.010

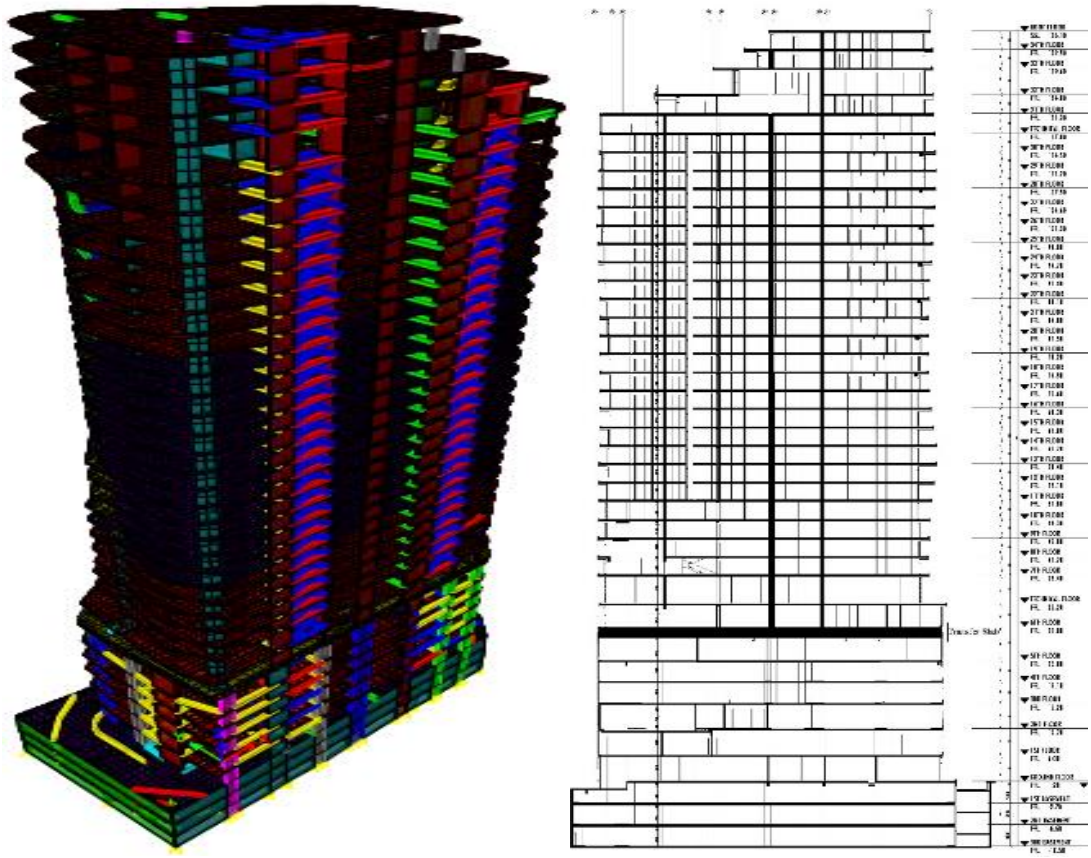

Fig. 3. 3D Model of the building and cross-section elevation.

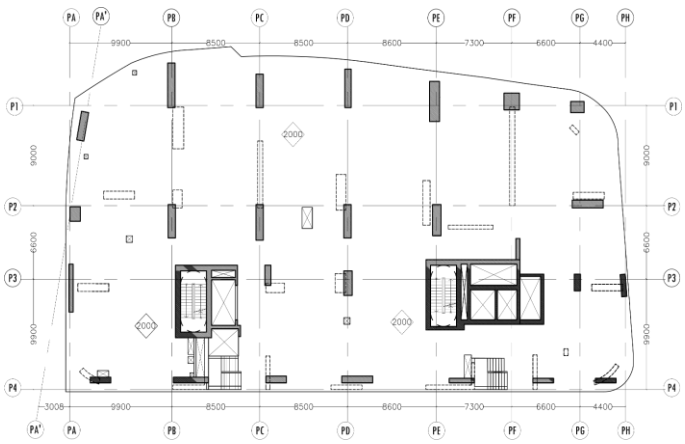

Fig.4. Layout of Transfer Slab and Below Columns.

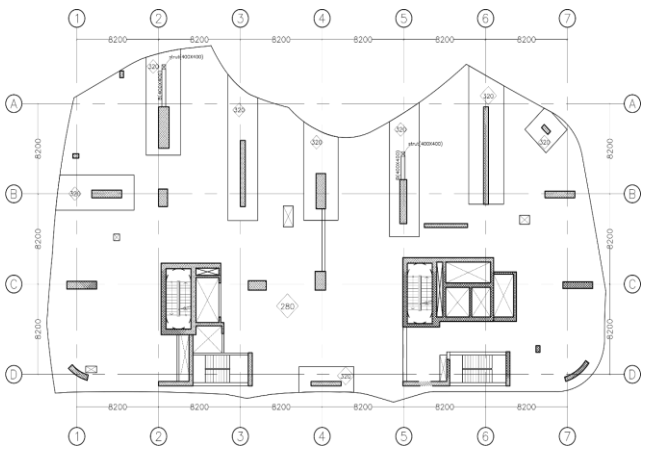

Fig. 5. Layout of Columns above Transfer Slab.

Calculated Results

Figures 6-9 show the story shear, moment, drift, and displacement in X- and Y-directions obtained using RS and TH methods.

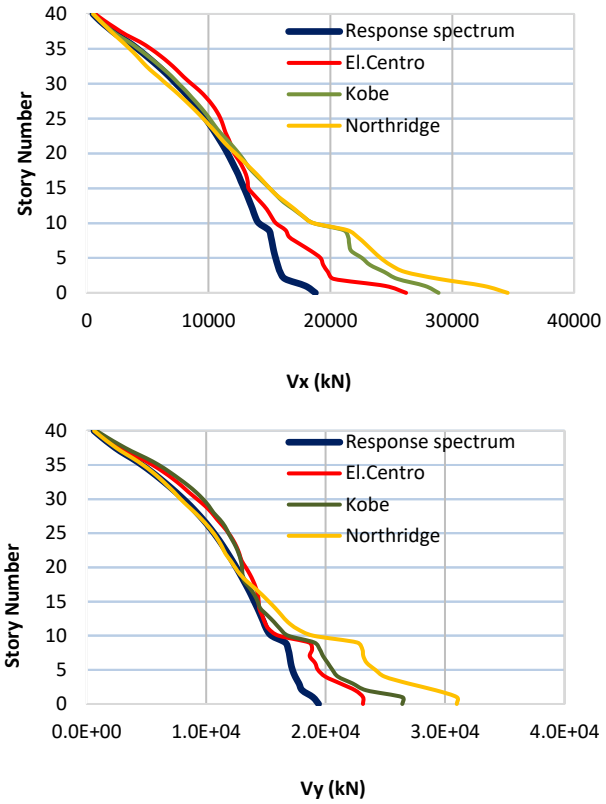

Fig. 6. Story shear in X- and Y-directions.

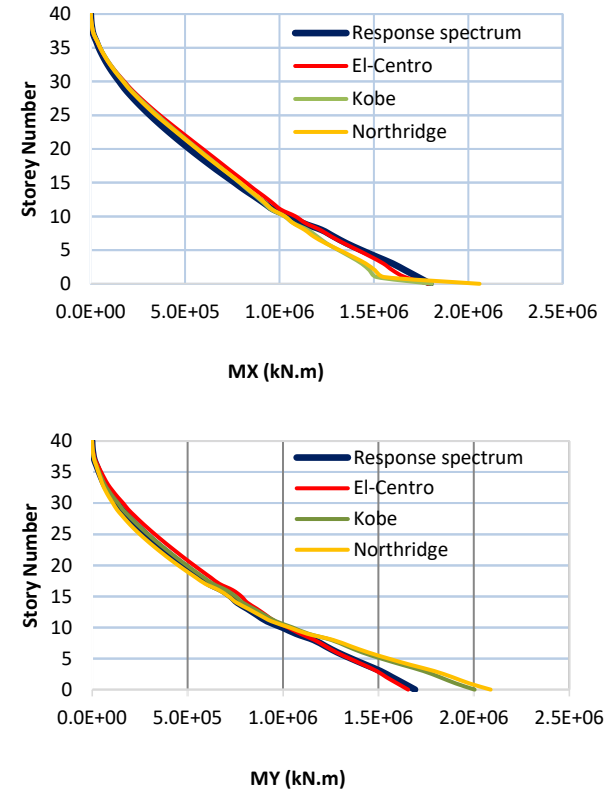

Fig. 7. Story moment in X- and Y-directions.

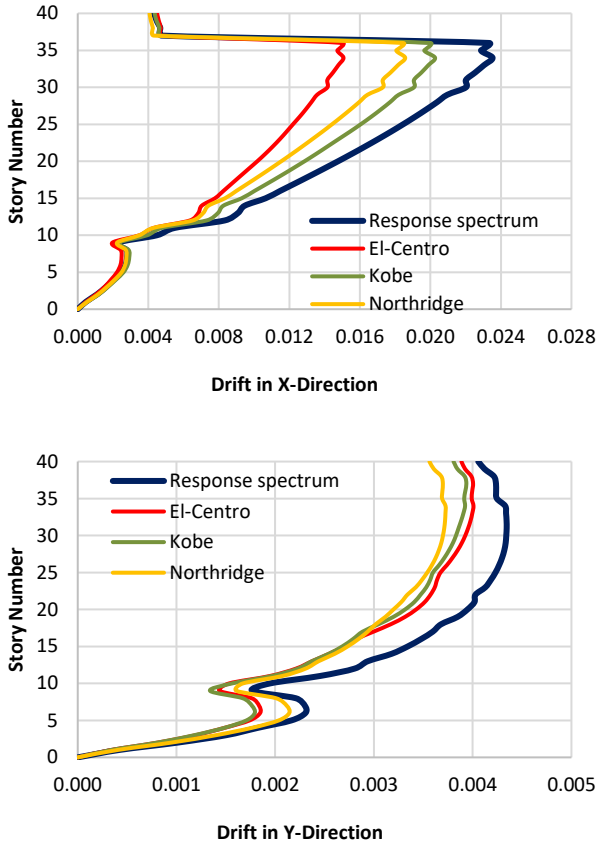

Fig. 8. Story drift in X- and Y-directions.

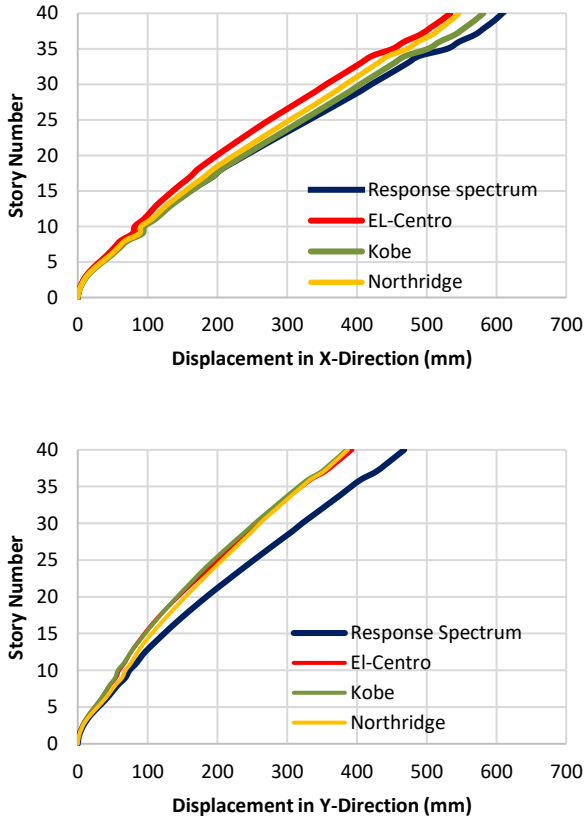

Fig. 9. Story displacement in X- and Y-directions.

The calculated results indicated that:

- The base shears in X- and Y-directions obtained using time-history analysis for El Centro, Kobe and Northridge earthquakes are about 1.33, 1.49 and 1.76 of that calculated using response spectrum analysis.
- The base moments in X- and Y-directions obtained using time-history analysis for El Centro, Kobe and Northridge earthquakes are about 0.99, 1.09 and 1.19 of that calculated using response spectrum analysis.
- There is an abrupt change in the lateral stiffness (story drift) in the vicinity of transfer floor.
- The structure top displacements in X- and Y-directions from time-history analysis is about 0.88 of the displacement from RS analysis.

Performance points

The POA was conducted using Eurocode 8-2004 target displacement method as shown in Fig. 10. It is worth mentioning here that, the as-build reinforcements' details for beams, columns, shear, and core walls are modeled in ETABS. It was found that most of the plastic hinges in X- and Y-directions are formed from O "Operational" to IO "Immediate Occupancy" performance level. Therefore, there is no significant damage would occur to the building and the structure can retain its original strength and stiffness.

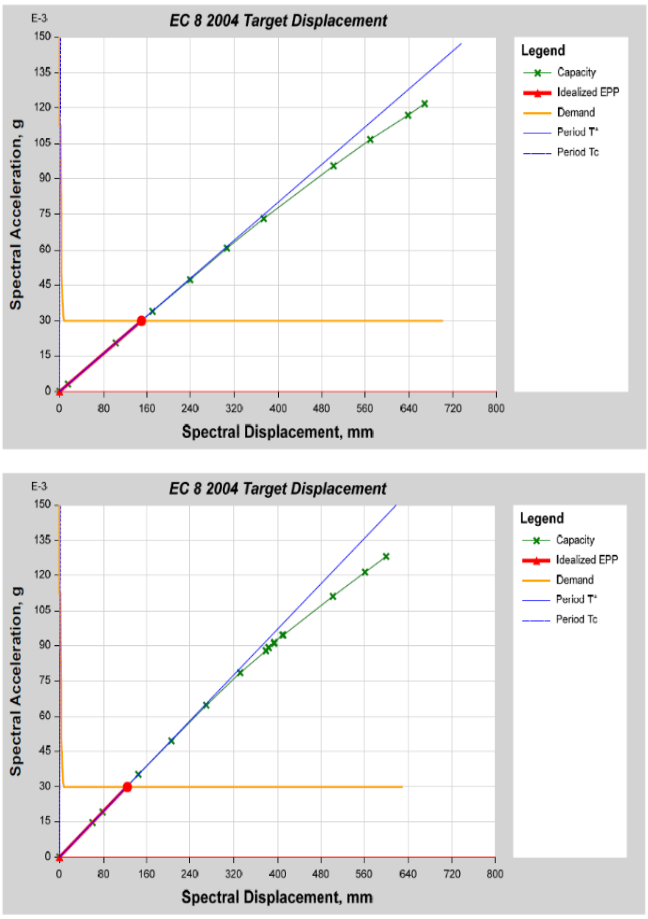

Fig. 10. Performance points in X- and Y-directions.

Comparison between numerical results

The numerically calculated base shear, displacement, story drift, and time period of the building are shown in Table 4. It is observed that base shear obtained using POA is about 64% and 71% of the static value in X- and Y-directions, respectively. Consequently, the building has a large safety margin till reaches its ultimate capacity.

Table 4. Building response in X- and Y-directions.

Building response	Static	RS	POA	TH
X-direction				
Base shear (kN)	27321	18771	17536	34547
Base moment (kN.m)	2806431	1799128	1570399	2059551
Top displacement (mm)	844	609	225	581
Period (sec)	6.4	6.4	4.49	6.4
Y-direction				
Base shear (kN)	27321	19412	18210	30977
Base moment (kN.m)	2868005	1692302	1387613	2088420
Top displacement (mm)	565	468	207	394
Period (sec)	6.4	6.4	4.07	6.4

5.2 Study Case No. 2

This case study is a RC building located in Riyadh, KSA with 17 stories and a total height of 64m above the ground level. The developed 3D model is shown in Fig. 11. The main system resisting the lateral loads is the building frame system. The transfer girder exists on the ground floor which is zero% of the building's total height. The columns below and above transfer girders are shown in Figures (12 and 13). The dimensions of transfer girders were 1800 mm x 1700 mm, and the bottom and top reinforcement were 68T25 and 34T25, respectively. The concrete compressive strength for horizontal and vertical elements were 40 MPa and 50 MPa, respectively. The yield stress for steel reinforcement was 420 MPa. The building was designed according to SBC301 and SBC304.

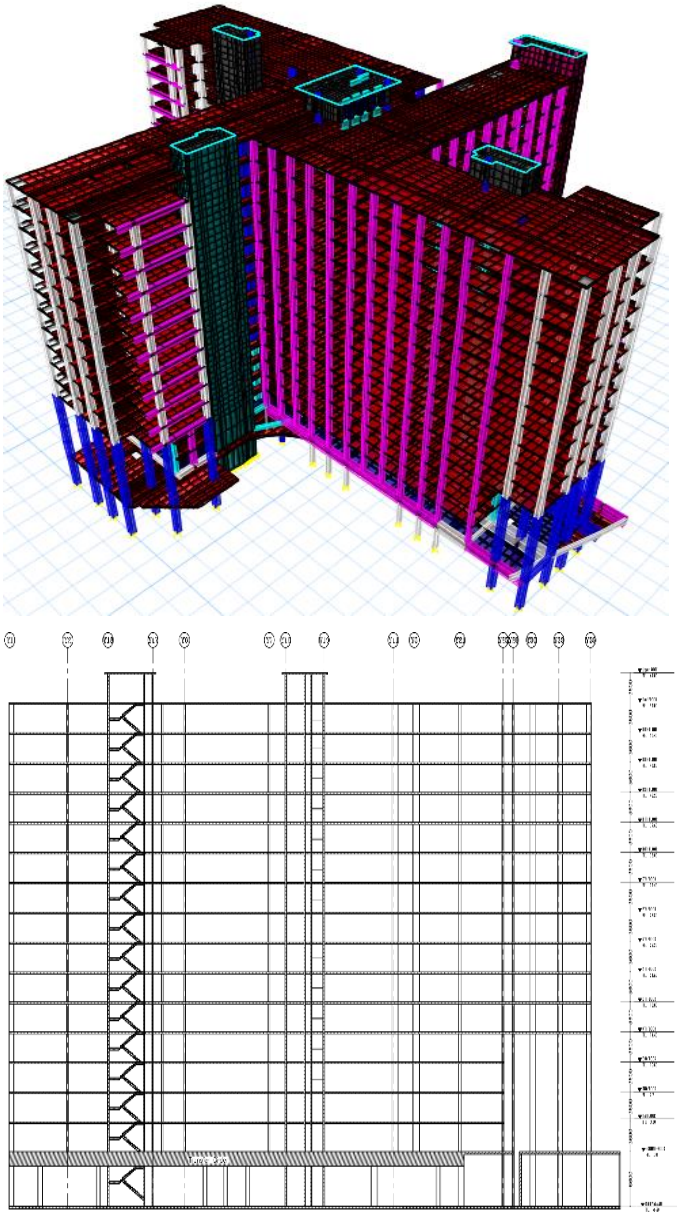

Fig. 11. 3D Model with transfer girders at 10% of total height and cross-section elevation.

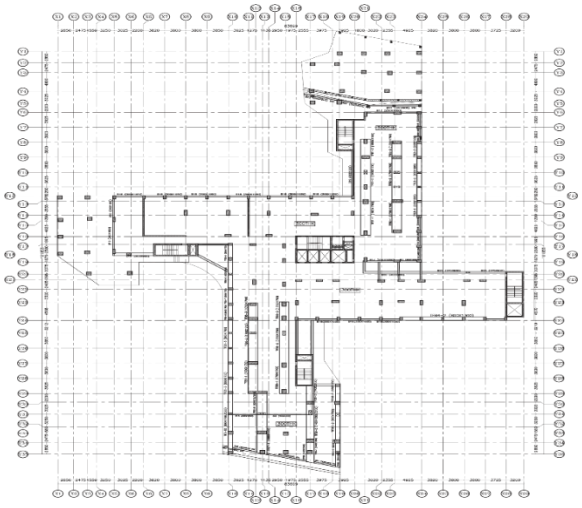

Fig.12. Layout of Transfer Girder and Below Columns.

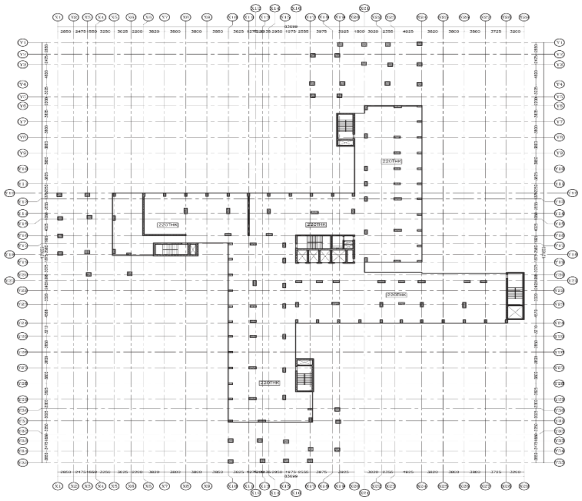

Fig.13. Layout of Columns above Transfer Girder.

Output results

Figures 14-17 show the calculated results of the global structural behavior in X- and Y-directions obtained using RS and TH methods.

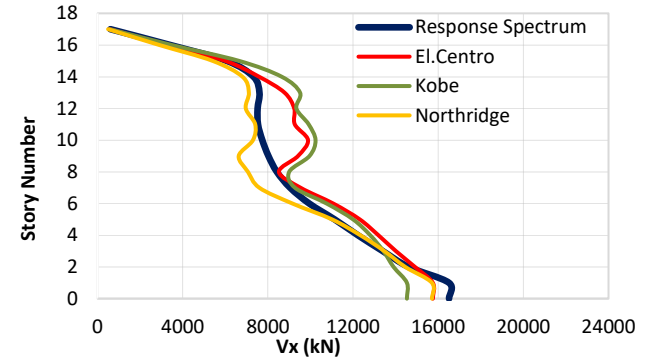

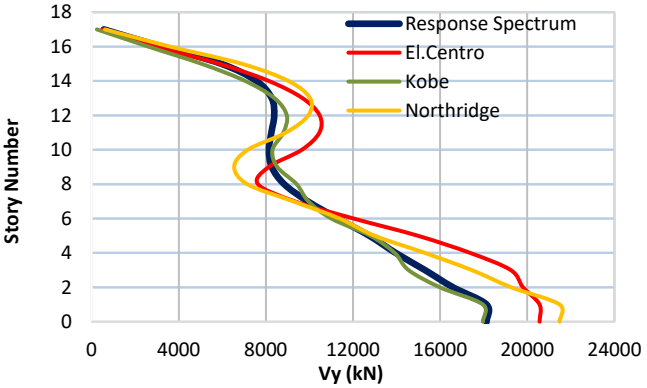

Fig. 14. Story shear in X- and Y-directions.

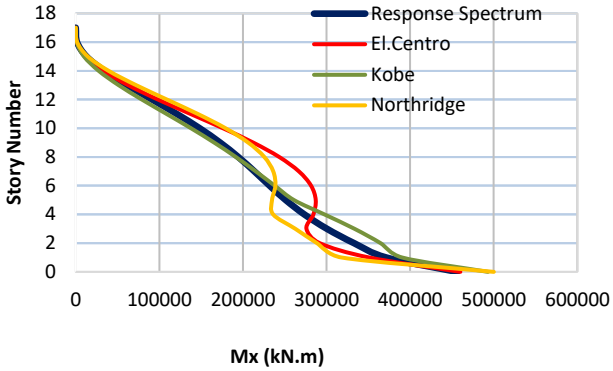

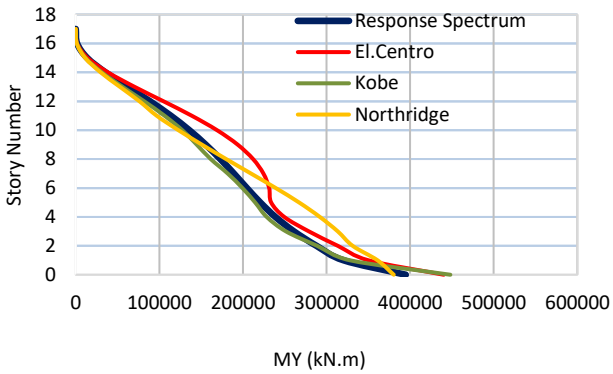

Fig. 15. Story moment in X- and Y-directions.

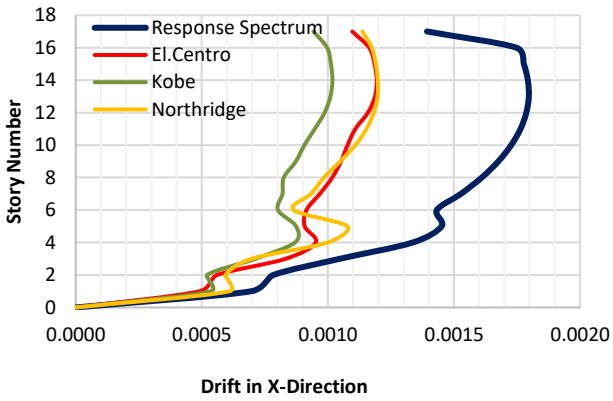

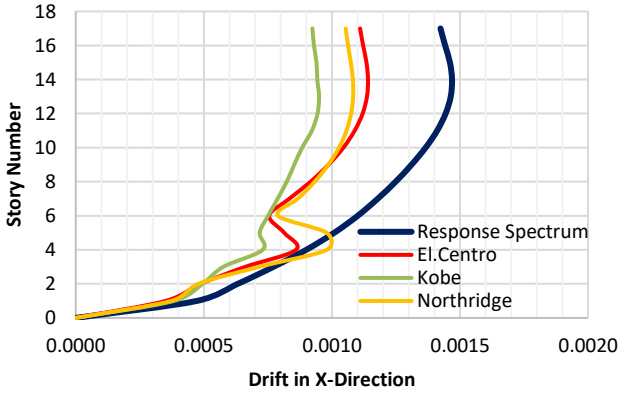

Fig. 16. Story drift in X- and Y-directions.

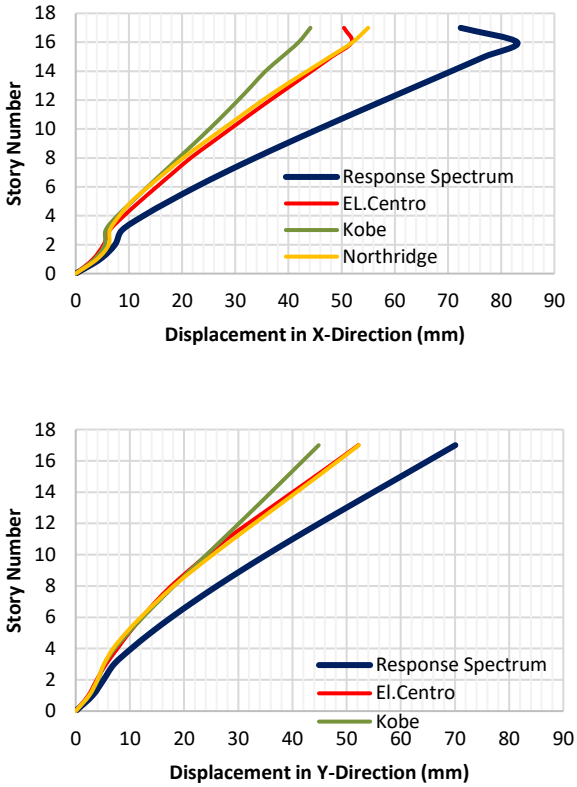

Fig. 17. Story displacement in X- and Y-directions.

The calculated results indicated that:

- The base shears in X- and Y-directions obtained using time-history analysis for El Centro, Kobe and Northridge earthquakes are about 1.04, 0.94 and 1.07 of that calculated using response spectrum analysis.
- The base moments in X- and Y-directions obtained using time-history analysis for El Centro, Kobe and Northridge earthquakes are about 1.06, 1.11 and 1.03 of that calculated using response spectrum analysis.
- There is an abrupt change in the lateral stiffness (story drift) in the vicinity of transfer floor.
- The structure top displacements in X- and Y-directions from time-history analysis is about 0.72 of the displacement from RS analysis.

Performance points

The analysis of pushover analysis is conducted using ASCE41-13 with displacement modification method as shown in Fig. 18. It was found that, majority of the plastic hinges in X- and Y-directions are formed from A to IO "Immediate Occupancy" performance level. Therefore, there is no significant damage would occur to the building and the structure can retain its original strength and stiffness.

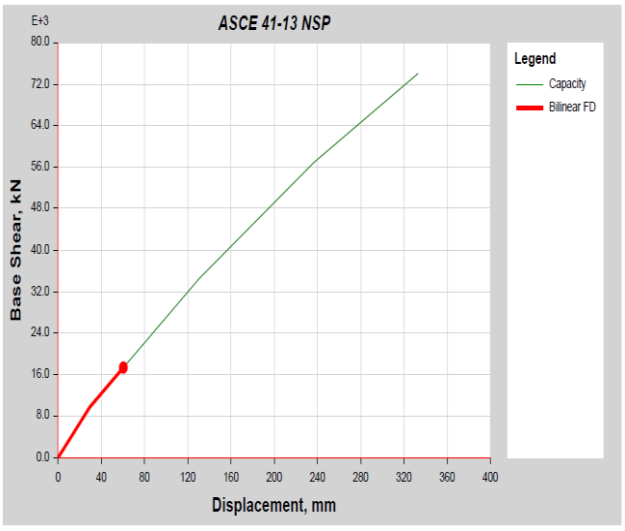

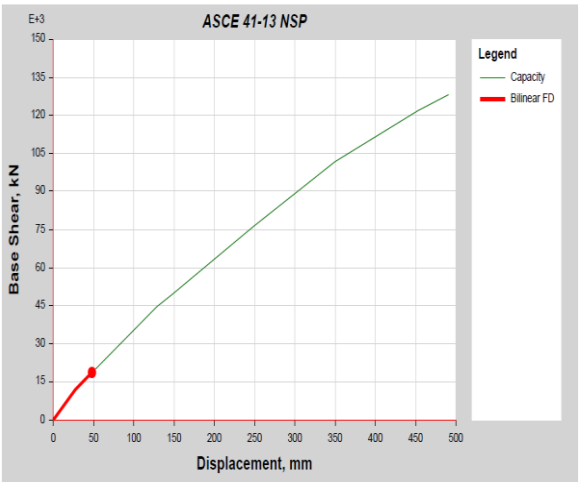

Fig. 18. Performance points in X- and Y-directions.

Comparison between numerical results

The numerically calculated base shear, displacement, drift, and time period values of the building are shown in Table 5. It is depicted that base shear obtained using POA is about 50% and 58% of the static value in X- and Y-directions, respectively. So, the building has a large safety margin till reaches its ultimate capacity.

Table 5. Building response in X- and Y-directions.

Building response	Static	RS	POA	TH
		X-direction		
Base shear (kN)	24821	16507	12437	15748
Base moment (kN.m)	1159029	456174	324729	500158
Top displacement (mm)	182	72	40	55
Period (sec)	1.64	3.16	2.20	3.16
		Y-direction		
Base shear (kN)	24821	18130	14420	21481
Base moment (kN.m)	1174573	394756	312512	440232
Top displacement (mm)	115	70	35	52
Period (sec)	1.64	3.16	1.96	3.16

5.3 Study Case No. 3

This case study is a reinforced concrete building located in Dubai, UAE with 52 levels and a total height of 195.30m above the ground level. Figure 18 shows the developed 3D model. The lateral load resisting system was the bearing wall system. The columns below and above transfer slab are shown in Figs. 19-20. The transfer slab thickness was 2800m and located at the 12th level representing 28% of the building's total height. Concrete compressive strength for both horizontal and vertical elements were 50 MPa and 70 MPa, respectively. The yield stress for steel reinforcement was 460 MPa. The building was designed according to (UBC 97, 1997).

Calculated results

Figures 21-22 show the results of the global structural behavior in X- and Y-directions obtained using RS and TH methods.

The calculated results indicated that:

- The base shears in X- and Y-directions obtained using time-history analysis for El Centro, Kobe and Northridge earthquakes are about 1.10, 1.07 and 1.01 of that calculated using response spectrum analysis.
- The base moments in X- and Y-directions obtained using time-history analysis for El Centro, Kobe and Northridge earthquakes are about 1.23, 130 and 0.85 of that calculated using response spectrum analysis.
- There is an abrupt change in the lateral stiffness (story drift) in the vicinity of transfer floor.
- The structure top displacements in X- and Y-directions from time-history analysis is about 0.91 of the displacement from RS analysis.

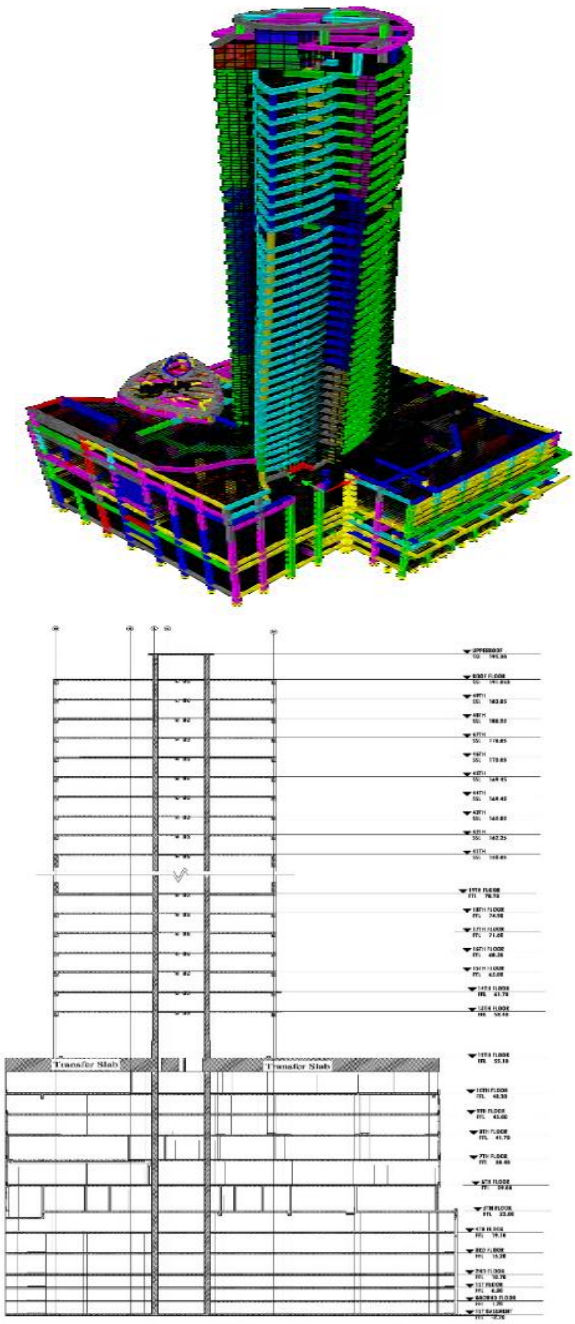

Fig. 18. 3D Model with Transfer Slab at 21% of total height and cross-section elevation.

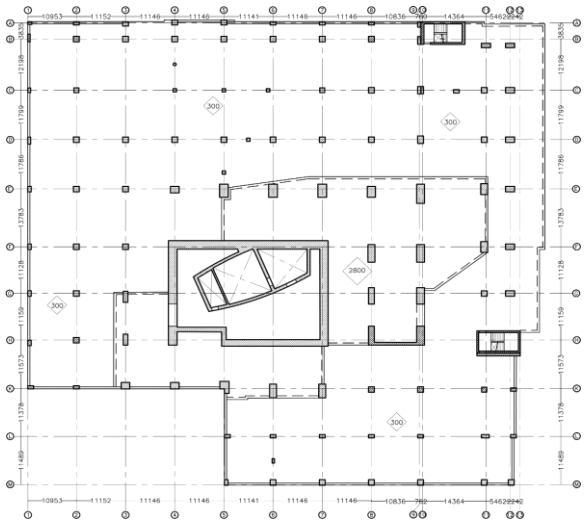

Fig.19. Layout of Transfer Slab and Below Columns.

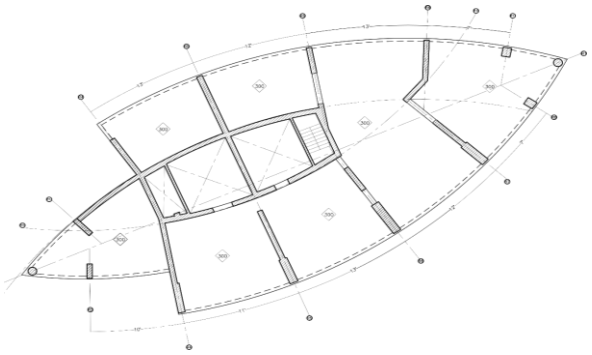

Fig.20. Layout of Columns above Transfer Slab

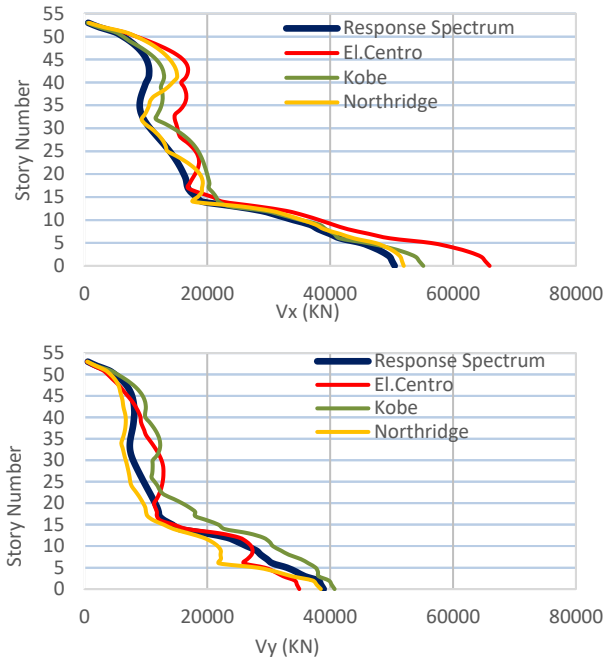

Fig. 21. Story shear in X- and Y-directions.

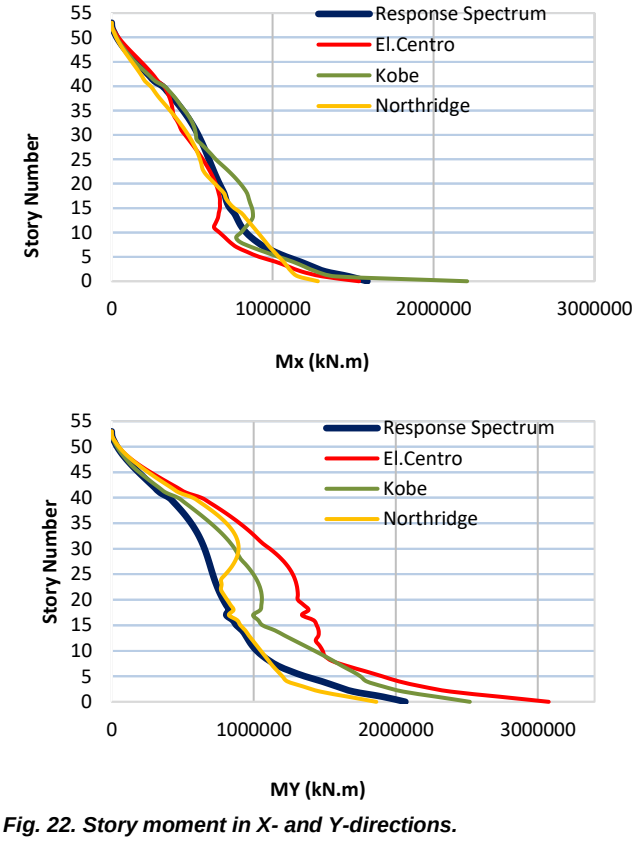

Fig. 22. Story moment in X- and Y-directions.

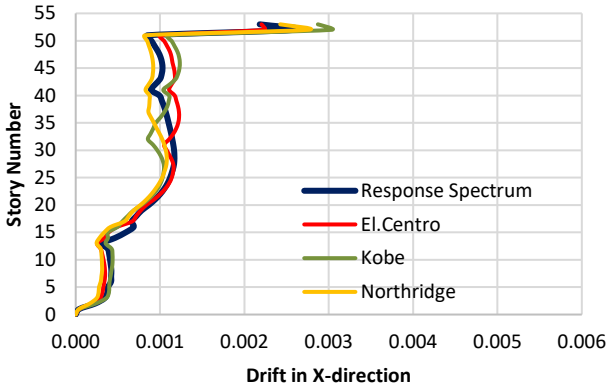

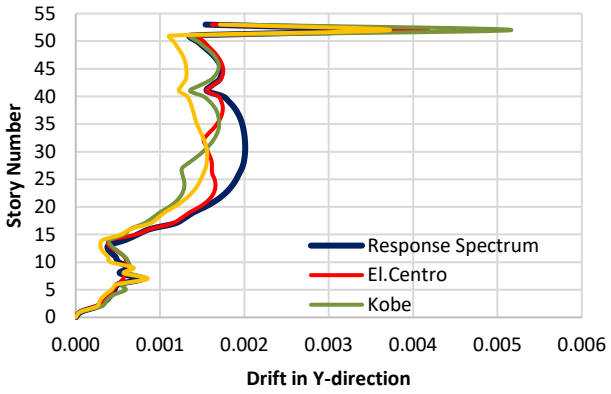

Fig. 23. Story drift in X- and Y-directions.

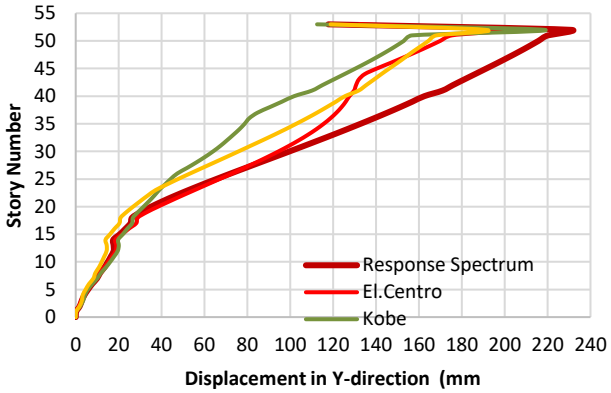

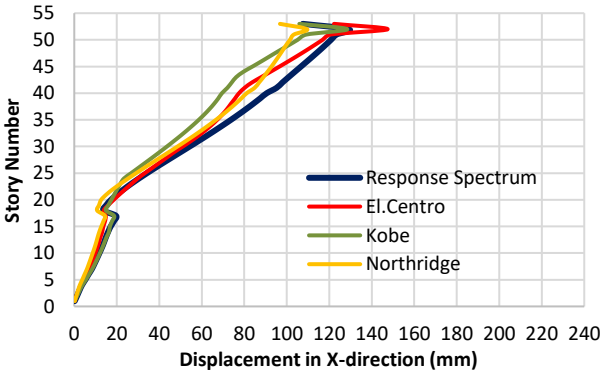

Fig. 24. Story displacement in X- and Y-directions.

Performance points

The analysis of pushover analysis is conducted using ASCE41-13 with displacement modification method. The calculated performance points in X- and Y-directions are shown in Fig. 25. It was found that most of the plastic hinges in X- and Y-directions are formed from O "Operational" to IO "Immediate Occupancy" performance level. Therefore, there is no significant damage would occur to the building and the structure can retain its original strength and stiffness.

Comparison between numerical results

The numerically calculated base shear, displacement, drift, and time period values of the building are shown in Table 6. It is highlighted that base shear obtained using POA is about 83% and 70% of the static value in X- and Y-directions, respectively. Therefore, the building has a large safety margin till reaches its ultimate capacity.

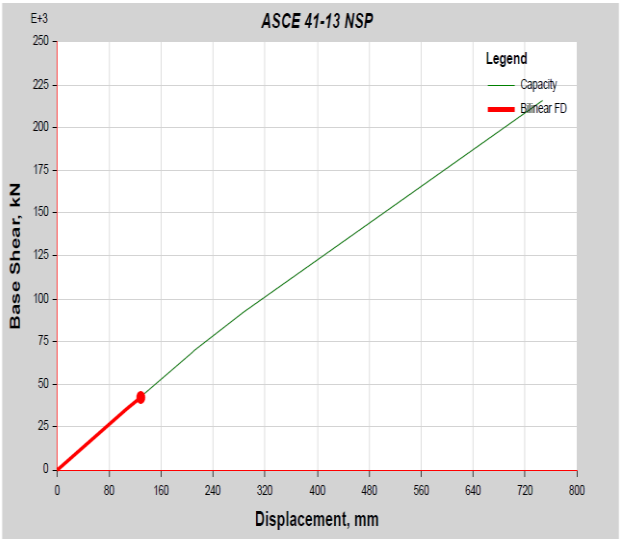

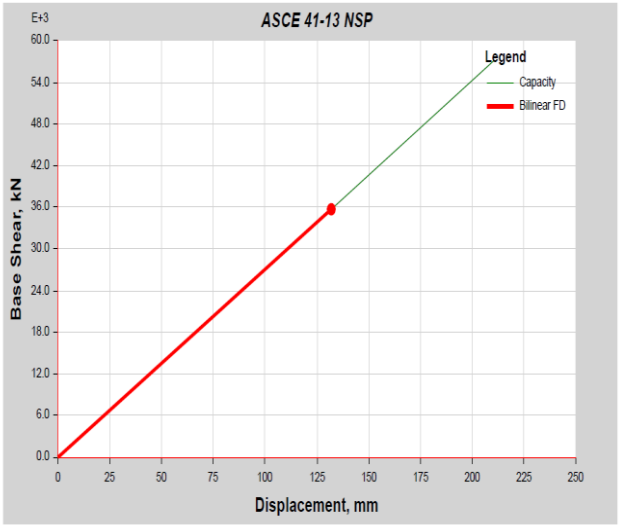

Fig. 25. Performance point in X- and Y-directions.

Table 6. Building response in X- and Y-directions.

Building response	Static	RS	POA	TH
		X-direction		
Base shear (kN)	51046	50505	42353	65950
Base moment (kN.m)	7280373	1588295	808301	2208191
Top displacement (mm)	615	109	56	129
Period (sec)	3.12	6.30	2.70	6.30
		Y-direction		
Base shear (kN)	51046	38957	35780	40733
Base moment (kN.m)	6984208	2067827	1345277	3077043
Top displacement (mm)	887	118	132	132
Period (sec)	3.12	6.30	3.72	6.30

6. Response Modification Factor

The response modification factor (R) is the factor that should be used to reduce the actual base shear force to get the design lateral force. Evaluation of R is based on the idealized-pushover curve to obtain the values of design shear (V_d), yield shear (V_y), ultimate shear (V_u), yield displacement (Δ_y), and ultimate displacement (Δ_u). The R values for the four studied cases are calculated using the following two methods:

6.1 ATC-63 Method

ATC-63 [21] proposed the following equation to calculate the value of R.

$$R = \Omega . R_\mu . R_R . R_\xi \quad (3)$$

Where Ω is the over strength factor, Rμ is the ductility factor, R_ξ is the damping factor and RR is the redundancy factor.

Table 7 shows the calculated values of response reduction factor. Where V_u is the ultimate base shear, V_d is the design base shear, T is the fundamental time period, Δ_u is the roof displacement from pushover curve calculated based on peak load, Δ_y is the yield displacement calculated based on equivalent elasto-plastic yield as recommended by (Park & Paulay, 1988), and Rμ is function of μ depends on time period as per (Newmark & Hall, 1982).

$$R_\mu = \begin{cases} 1 & if \quad T < 0.2 \\ \sqrt{2\mu - 1} & 0.2 < T < 0.5 \\ \mu & T > 0.5 \end{cases} \quad (4)$$

6.2 FEMA 356 Method

FEMA356 [13] gives the following equation to calculate the response reduction factor:

$$R = \frac{S_a}{V_y/_W} . C_m \quad (5)$$

Where W is the effective seismic weight, Vy is the yield strength, Sa is the response spectrum acceleration at the fundamental period and damping ratio of the building in the considered direction, and Cm is the effective mass factor.

Table 8 presents the calculated values of response reduction factor. Figure 26 shows the nonlinear force-displacement relationship between base shear and displacement of the control node that shall be replaced with an idealized relationship to calculate the effective lateral stiffness (Ke), effective yield strength (Vy), post-yield slope (α), and elastic lateral stiffness (Ki).

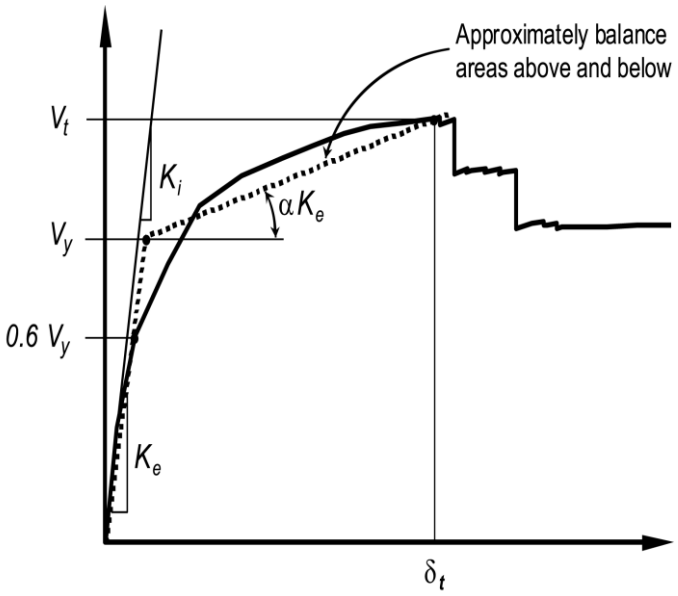

Fig. 26. Idealized force-displacement curves (FEMA-356, 2000).

The results shown in Tables 7 and 8 indicated the followings:

- For study cases No. 1 and 3 having transfer slabs, the calculated response modification factor "R" in both directions calculated using ATC-63 or FEMA 356 are greater than the values of 5.0 and 4.50 that allocated in design code ECP 201 and UBC 97, respectively. This means that the structure has a higher ductility and ability for earthquake energy dissipation upon its nonlinear behavior and its members ultimate capacity.
- For study case No. 2 with transfer girders, the calculated response modification factor "R" in both directions calculated using ATC-63 or FEMA 356 are smaller than the values of 5.0 and 5.50 that allocated in design code ECP 201 and SBC 301, respectively. This means that the structure has a lower ductility and ability for earthquake energy dissipation upon its nonlinear behavior and its members ultimate capacity.

Table 7. Response modification factor in X-and Y-directions.

Study case No.	V_u (kN)	V_d (kN)	T (sec)	$\Omega = V_u/V_d$	Δ_u (mm)	Δ_y (mm)	$\mu = \Delta_u/\Delta_y$	R_μ	R
X-direction									
1	73256	27321	6.40	2.68	1000	433	2.31	2.31	6.19
2	73968	24821	3.16	2.98	333	237	1.41	1.41	4.19
3	215617	51046	6.30	4.22	747	286	2.61	2.61	11.03
Y-direction									
1	80000	27321	6.40	2.93	1000	427	2.34	2.34	6.86
2	128255	24821	3.16	5.17	491	249	1.97	1.97	10.19
3	57154	51046	6.30	1.12	211	45	4.69	4.69	5.25

Table 8. Response modification factor in X- and Y-directions.

Case study No.	S_a (g)	W (kN)	T_i (sec)	K_i (kN/m)	K_e (kN/m)	$T_e = T_i\sqrt{\frac{K_i}{K_e}}$ (sec)	V_y	C_m	R
X-direction									
1	0.095	1834077	4.50	78133	78133	4.50	33853	1	5.15
2	0.029	1777263	2.33	322755	296992	2.43	9850	1	5.23
3	0.038	5189829	2.69	330851	330851	2.69	35574	1	5.54
Y-direction									
1	0.104	1834077	4.08	88373	88373	4.08	37737	1	5.05
2	0.029	1777263	3.16	418363	334372	2.35	11995	1	4.30
3	0.022	5189829	3.27	271991	271991	3.27	21699	1	5.26

7. Conclusions

The seismic behavior of high-rise buildings with transfer slabs and transfer girders was numerically investigated. Four constructed case studies are analyzed using response spectrum, time history and pushover analysis methods. Based on the obtained results, the following conclusions may be drawn:

The story shear force is significantly reduced above the transfer floor location due to the abrupt decrease in deployed mass.

For the studied cases, there is an abrupt change in their lateral stiffness in the vicinity of the transfer floor. Therefore, the transfer floor location controls the maximum location for the story drift. It is advisable to locate the transfer floor in the range of 20% to 30% of the building's height.

In order to obtain the required participation mass ratios, buildings with transfer elements at lower level should be analyzed using a greater number of modes to reach the required 90% of mass participation.

For the sake of considering the effect of deformations of transfer slabs in the seismic behavior of the buildings, it is recommended to model the transfer slab using thick shell elements or three-dimensional solid elements and consider it as a semi-rigid diaphragm as transfer elements attract considerable lateral loads, thus they must be designed accordingly.

For the case studies presented in this work, base shear obtained using pushover analysis is about 50% to 83% of the static Approach. Consequently, using POA could save a considerable amount of concrete volume and reinforcement quantity of the buildings.

The pushover analysis can predict the degradation of structure stiffness, the formation and locations of plastic hinges as lateral loads increase. Also, POA can identify members that are likely to reach critical states during an earthquake, hence evaluating the building's performance to the considered earthquake. The studied four buildings have a large safety margin till reach their ultimate capacity.

The response modification factor is very sensitive to both horizontal and vertical irregularity. For the studied cases in this research, the R values given in the building codes were overestimated for the cases with transfer slabs and underestimated for cases with transfer girders.

References

Abdelbasset, Y. M., Sayed-Ahmed, E. Y. & Mourad, S. A., 2014. *High-Rise Buildings with Transfer Floors: Drift Calculations.* Madrid, s.n., pp. 637-644.

Abdul Sameer, M. & Azeem, M. A., 2019. A Study on Seismic Performance of Tall Buildings with Transfer Plate. *International Journal of Applied Engineering Research,* 14(8), pp. 1849-1859.

Applied Technology Council & Federal Emergency Management Agency, 2008. *Quantification of Building Seismic Performance Factors: ATC-63 Project Report,* Redwood: Applied Technology Council.

ASCE 7, 1., 2010. *Minimum Design Loads for Buildings and Other Structures,* Virginia: American Society of Civil Engineers.

ATC 40, 1996. *Seismic Evaluation and Retrofit of Reinforced Concrete Buildings,* Washington, D.C.: Applied Technology Council.

Ayash, N. M., Hanna, N. F. & Hamdy, A., 2020. Study of the Seismic Response of R.C. High-Rise Buildingns with Double Transfeer Floors. *Journal of Engineering and Applied Science,* 67(5), pp. 1117-1136.

Egyptian Code of Practice (ECP 201), 2012. *Calculation of Loads and Forces on Structures and Building,* Cairo: Housing and Building National Research Center.

Egyptian Code of Practice (ECP 203), 2020. *Design and Construction of Reinforced Concrete Structures,* Cairo: Housing and Building National Research Center.

Elassaly, M. & Nabil, M., 2017. Seismic Damage Assessment of RC Building with the Transfer Slab System. *Earthquake Resistant Engineering Structures,* 172(XI), pp. 83-95.

Elawady, A. K., Abdelrahman, A. A. & Sayed-Ahmed, E. Y., 2014. Seismic Behaviour of High-Rise Buildings with Transfer Floors. 14 2.pp. 57-70. doi: https://doi.org/10.56748/ejse.14181

Eurocode 8 (EC8-1), 2004. *Design of structures for earthquake resistance. Part 1: General rules, seismic actions and rules for buildings.,* Brussels, Belgium: European Committee for Standardization.

FEMA-356, 2000. *Prestandard and Commentray for the Sesimic Rehabilitation of Buidings,* California: Federal Emergency Management Agency.

FEMA-440, 2005. *Improvement of Nonlinear Static Seismic Analysis Procedures.* California: Federal Emergency Management Agency.

Freeman , S. A., Nicoletti , J. P. & Tyrell , J. V., 1975. *Evaluation of existing buildings for seismic risk-acase study of Puget Sound Naval Shipyard.* Bremerton, Washington, s.n.

Hakim, R. A., Alama, M. S. & Ashour, S. A., 2014. Seismic Assessment of RC Building According to ATC 40, FEMA356 and FEMA 440. *Arab J Sci Eng,* Volume 39, p. 7691–7699.

Londhe, S. R., 2011. Shear strength analysis and prediction of reinforced concrete transfer beams in high-rise buildings. *Structural Engineering and Mechanics,* 37(1), pp. 39-59.

Newmark, N. M. & Hall, W. J., 1982. *Earthquake spectra and design.* Oakland: Earthquake Engineering Research Institute.

Osman, A. & Abdel Azim, M., 2015. *Analysis and Behavior of High-rise Buildings with Transfer Plate System.* Algeria, s.n.

Park, R. & Paulay, T., 1988. *Reinforced Concrete Structures.* New York: Wiley.

PeerDatabase,2006.*http://peer.berkeley.edu/smcat/.* [Online].

Saudi Buiding Code National Committee, 2007. *Concrete Structures,* Riyadh: Saudi Building Code.

Saudi Building Code National Committee , 2007. *Loads and Forces Requirements.* Riyadh: Saudi Building Code.

Stefano, M. D. & Mariani, V., 2014. *Pushover Analysis for Plan Irregular Building Structures.* s.l.:s.n.

UBC 97, 1997. *Uniform Building Code,* Whittier, California: International Conference of Building Officials.

Yacoubian, M., Lam, N., Lumantarna, E. & Wilson, J. L., 2017. *Seismic Performance Assessment of Structural Walls Supporting Towers in Tall Buildings.* Canberra, s.n., pp. 1-11.